VOLUME 81 SEPARATE No. 677

PROCEEDINGS

AMERICAN SOCIETY
OF
CIVIL ENGINEERS

APRIL, 1955

VESSELS PARTIALLY SUPPORTED BY SOIL

by W. A. Boothe, R. T. Gray,
and G. Horvay

ENGINEERING MECHANICS
DIVISION

{Discussion open until August 1, 1955}

Headquarters of the Society
33 W. 39th St.
New York 18, N. Y.

PRICE $0.50 PER COPY

THIS PAPER

--represents an effort by the Society to deliver technical data direct from the author to the reader with the greatest possible speed. To this end, it has had none of the usual editing required in more formal publication procedures.

Readers are invited to submit discussion applying to current papers. For this paper the final date on which a discussion should reach the Manager of Technical Publications appears on the front cover.

Those who are planning papers or discussions for "Proceedings" will expedite Division and Committee action measurably by first studying "Publication Procedure for Technical Papers" (Proceedings – Separate No. 290). For free copies of this Separate—describing style, content, and format—address the Manager, Technical Publications, ASCE.

This paper was published at 1745 S. State Street, Ann Arbor, Mich., by the American Society of Civil Engineers. Editorial and General Offices are at 33 West Thirty-ninth Street, New York 18, N. Y.

VESSELS PARTIALLY SUPPORTED BY SOIL

W. A. Boothe,[1] R. T. Gray,[2] and G. Horvay[3]

ABSTRACT

Curves are plotted which indicate the reduction in bending stresses that can be achieved near a discontinuity in a cylindrical shell by application of partial elastic support in the vicinity of the discontinuity.

INTRODUCTION

Cylindrical pressure containers occasionally are supported by encasing their bottom portion in concrete. In order to reduce the bending stresses that develop at the interface where built-in and free portions join, some manufacturers have adopted the practice of introducing a transition zone of partial restraint. Sand of suitable stiffness dammed up to a depth of several shell attenuation lengths forms a buffer layer, and splits the single interface—the juncture of built-in and free zone—into two interfaces; the juncture $\overline{10}$ of built-in and partially restrained zone, and the juncture $\overline{21}$ of partially restrained and free zone, as illustrated in Fig. 1. The question arises: By what factor is the bending stress reduced through the introduction of this buffer zone? We shall show that when the sand layer is regarded as having a spring constant κ uniform over its depth, a proper choice of κ will result in a reduction of the maximum bending stress to 2/9 of the value encountered when no transition zone is provided. If we also take the variation of κ, from 0 at the surface to κ_{max} at the bottom, into account, then, naturally, the transition becomes much smoother, and by making κ_{max} very large (and having an adequate distance D available) the bending stresses may be reduced to arbitrarily small values. Needless to say, a similar buffer zone action can be provided not only by sand restraint but also by the use of closely spaced metal reinforcing rings as indicated in Fig. 2.

The contents of this paper are as follows: First we establish the formula for sand stiffness in terms of its more familiar characteristic, compressibility; we also give the formula for metal band stiffness. Then we write the expressions for the membrane behavior of the shell in each of the Zones 0, 1, 2, considering the shell to be cut along the interface between each zone. Third, we determine the edge moments and edge shears developed at the interfaces

1. Formerly, Member, Advanced Engineering Program, General Electric Co.; at present, Development Engineer, General Engineering Laboratory, G.E. Co., Schenectady, N.Y.
2. Formerly, member, Advanced Engineering Program, General Electric Co.; at present, Development Engineer, Major Appliances Division, G.E. Co., Erie, Pa.
3. Development Engineer, Knolls Atomic Power Lab.[4] Ao 1072 Schenectady, N.Y.
4. The Knolls Atomic Power Laboratory is operated by the General Electric Co. for the Atomic Energy Commission. The work reported here was carried out under contract No. W-31-109 Eng.-52.

which maintain continuity between the shell sections in the three zones. Fourth, we calculate the stresses and deformations produced by the edge reactions, and superpose these effects on the membrane results. The final results are the curves drawn in Fig. 5 for radial displacement δ, and in Fig. 6 for meridional stress σ_x versus position $n\ell_1$ (counted from interface) for values 0, 1, 10, and ∞ of the spring constant ratio

$$\rho = \kappa / k \tag{1a}$$

Here

$$k = Eh/R^2 \quad psi/in \tag{1b}$$

is the familiar stiffness expression of a shell of radius R and wall thickness h, and κ is the soil stiffness, psi/in.; ℓ_i is the attenuation length, as given by Equation (24), for Zone i; n is the number of attenuation lengths along the shell from the interface in question.

The stresses plotted are given in units of

$$\sigma_p = pR/h \tag{2}$$

where σ_p is the hoop stress in an unrestrained shell. The deformations plotted are given in units of

$$\delta_p = (1-\mu/2)R^2 p/Eh \tag{3}$$

where δ_p is the outward radial displacement in an unrestrained shell (sealed at the two ends). Similar curves also have been calculated (but are not shown) for 0.1, 2, and 100, as well as for the resultant hoop stress, σ_θ. For the Poisson ratio, μ, the value 0.3 was used.

The composite picture, Fig. 7, illustrates the main conclusions of the paper. Using subscripts i, 0 for inner and outer fiber, and subscripts $\overline{10}$, $\overline{21}$ to indicate action arising in the vicinity of interfaces $\overline{10}$ and $\overline{21}$, Fig. 7 plots the highest values of $\sigma_{x\overline{10}i}$, $\sigma_{x\overline{21}i}$, $\sigma_{\theta\overline{10}o}$, $\sigma_{\theta\overline{21}o}$ and the lowest values of $\sigma_{x\overline{10}o}$, $\sigma_{x\overline{21}o}$, $\sigma_{\theta\overline{10}o}$, $\sigma_{\theta\overline{21}o}$ versus ρ, as derived from Fig. 6 for and a similar (not shown) figure for σ_θ. All other σ_x and σ_θ stresses (such as the lowest value of $\sigma_{x\overline{10}i}$, or the highest value $\sigma_{\theta\overline{21}i}$ are intermediate to the upper and lower σ_x curves, and to the upper and lower σ_θ curves, respectively. Thus the heavy contour in Fig. 7 indicates the dependence of the stress range on the stiffness ratio ρ. It is seen that the inner fiber meridional stress at the interface $\overline{10}$ is the largest stress for stiffness ratios from $\rho = 0$ to $\rho = 2$; in this range $\sigma_{x\overline{10}i}$ decreases from 2.04 σ_p to 1.04 σ_p and the bending component of $\sigma_{x\overline{10}i}$ decreases from 1.54 σ_p to 0.54 σ_p. In the range $\rho = 2$ to $\rho = 16$ the hoop stress in the outer fiber near interface $\overline{21}$ is largest; it has an essentially constant value; $\sigma_{\theta\overline{21}o} = 1.04\ \sigma_p$. In the range $\rho = 16$ to $\rho = \infty$ the inner fiber meridional stress near interface $\overline{21}$ is the largest: $\sigma_{x\overline{21}i}$ rises from 1.04 σ_p to 2.04 σ_p.

We may refer to the range $\rho = 2$ to $\rho = 16$, where $\sigma_\theta = 1.04\ \sigma_p$ is the maximum stress, as the optimum range, and to the point $\rho = 3.8$ where $\sigma_{x\overline{10}i} = \sigma_{x\overline{21}i} = 0.83\ \sigma_p$ as the optimum point. For this value of ρ the maximum bending stress experienced by the shell is 0.33 σ_p, i.e., it is only about 1/4.5 of the maximum bending stress that develops when $\rho = 0$ or ∞.

Stiffness of Soil[5]

Stiffness of soil is usually specified in the form of an e - p curve as illustrated in Fig. 3a, derived from a compression test, illustrated in Fig. 3b. The soil sample is confined in a ring, and it is compressed by means of a rigid slab through the application of pressure p. Let e be the original void ratio of the soil, i.e. let

$$e = V_v / (V - V_v) \tag{4}$$

where V is the total volume of the sample, V_v the total volume of voids. Fig. 3a plots a typical curve showing the decrease in void with an increase in pressure. For the curve shown, the void change in the range from p = 0 to 150 psig is $\Delta e = 0.05$. If, as shown in Fig. 3b, the occupied volume is permitted to change only through a change in a single dimension, L, then we may write

$$\Delta e = \Delta V_v / (V - V_v) = \Delta L / (L - L_v) = (1+e)\Delta L / L \tag{5}$$

Consequently, the spring constant for the arrangement shown in Fig. 3b is

$$\kappa = \Delta p / \Delta L = \frac{1+e}{L} \frac{\Delta p}{\Delta e} \tag{6}$$

If the depth D of the sand layer in Fig. 1 is three or more times the width L, then the existence of a transition layer below the interface $\overline{21}$, about L deep, where the soil stiffness gradually increases from zero to its full value, κ, may be ignored (this is conservative). If the width L is small also in comparison with the shell radius R, then we may regard compression of the sand as a one-dimensional affair. It follows that for e = 0.8, Δp = 150 psi, Δe = 0.05, and a width L = 2 ft. of the sand layer (and assuming also $D \geq 3L$, $R >> L$), the soil provides a stiffness

$$\kappa = \frac{1.8}{24} \times \frac{150}{0.05} = 225 \text{ psi/in} \tag{7a}$$

Consider furthermore a pressure vessel of radius R = 20 ft. wall thickness h = 1 in. and modulus of elasticity E = 30 x 10^6 psi. Its stiffness is

$$k = 30 \times 10^6 \times 1 / 240^2 = 520 \text{ psi/in} \tag{7b}$$

Thus, for the foregoing numerical values, 520 psi pressure will expand the vessel 1 in. and 225 psi pressure will compress the sand layer 1 in. Consequently, ratio of soil stiffness to pressure vessel stiffness is

$$\rho = 225, 520 = 0.43 \tag{8}$$

Of course, one must be careful not to take the stiffness Equation (6)—which ignores nonlinearity, surface behavior, uneven compacting, pockets, change with atmospheric conditions, water-logging, etc.—too literally. If we wish to have a ratio $\rho = 4.3$, we can not, in practice, insure it by reducing L from 24 in. to 2.4 in., because, in pouring sand into such a narrow channel, we may no longer ignore the departures from assumed uniform behavior. But for a layer 2 ft. wide, and more than 4 ft. deep, we are justified in concluding from Fig. 7, abscissa $\rho = 0.43$, that the maximum stress in the container is

5. This section is based on Article 13 in "Soil Mechanics," by K. Terzaghi and R. B. Peck, Wiley and Sons, 1948. Fig. 3a represents conditions for dense sand.

$$\sigma_x = 1.6\,\sigma_p \tag{9}$$

of which 0.50 σ_p is meridional tensile stress caused by the pressure, and 1.1 σ_p is bending stress caused by the sudden change in restraint at the interface $\overline{10}$ where the concrete and the sand layer meet.

Stiffness of Metal Bands

The stiffness provided by thin-walled metal rings is well-known,

$$\varkappa = \gamma h_r E / R_r^2 \tag{10}$$

where h_r is the ring wall-thickness, R_r is the mean ring radius, and γ is the ring height t divided by the ring spacing s, as indicated in Fig. 2.

Membrane State

We consider the shell dissected at the interfaces $\overline{01}$ and $\overline{12}$, and let each section acquire its own membrane deformations and stresses under the inward pointing normal load Z, psi, as indicated in Fig. 4a. For Zone 1 this is

$$Z = \varkappa\delta - p \tag{11}$$

and leads to the hoop force per unit length of cylinder

$$N_\phi = h\sigma_\phi = -RZ \tag{12}$$

In the above δ is the radial outward displacement, σ_θ the hoop stress, and N_θ the hoop force. On the other hand, the meridional force and stress depend only on p,

$$N_x = h\sigma_x = Rp/2 = h\sigma_p/2 \tag{13}$$

Here σ_p, introduced earlier in Equation (2), is the pressure hoop stress in an unrestrained shell.

From the expression

$$\varepsilon_\phi = \delta, R = (N_\phi - \mu N_x)/Eh \tag{14}$$

of the hoop strain we eliminate δ by means of Equations (11), (12), and (13), and obtain

$$\sigma_\phi = N_\phi/h = \sigma_p(1+\mu\varsigma/2)/(1+\varsigma) \tag{15}$$

From Equations (13) and (14) it now follows that

$$\delta = (R^2 p/Eh)(1-\mu/2)/(1+\varsigma) = \delta_p/(1+\varsigma) \tag{16}$$

where δ_p, introduced earlier in Equation (3), is the radial displacement in an unrestrained shell. Placing $\rho = 0$ in these expressions we obtain the familiar formulas

$$\sigma_x = \sigma_p/2, \qquad \sigma_\phi = \sigma_p, \qquad \delta = \delta_p \tag{17}$$

which pertain to the unrestrained zone; placing $\rho = \infty$ we obtain

$$\sigma_x = \sigma_p/2, \qquad \sigma_\phi = \mu\sigma_p/2, \qquad \delta = 0 \tag{18}$$

which pertain to the fully restrained zone. We assumed that the concrete foundation prohibits radial expansion but does not prevent longitudinal stretching.

Edge Moments and Forces which Eliminate Misalignments

Henceforth we shall use subscripts m for the membrane results derived in the previous section, to distinguish them from the effects of edge load actions to be introduced in the following: In Fig. 4 we show the misalignments

$$\delta^*_{21} = \delta_{2m} - \delta_{1m} = \rho\delta_p/(1+\rho)$$
$$\delta^*_{10} = \delta_{10} - \delta_{0m} = \delta_p/(1+\rho) \qquad (19a, b)$$

in displacement which arise at interfaces $\overline{21}$ and $\overline{10}$ due to membrane action only. Since the membrane state gives rise to no rotations

$$\chi_{0m} = \chi_{1m} = \chi_{2m} = 0 \qquad (20)$$

there are not rotational misalignments,

$$\chi^*_{21} = \chi_{2m} + \chi_{1m} = 0$$
$$\chi^*_{10} = \chi_{1m} + \chi_{0m} = 0 \qquad (21)$$

Note that we consider a rotation χ positive if it rotates inward as viewed from the common edge, as shown in Fig. 4b. Likewise we regard shear force H as positive if it points outward as viewed from the common edge. On the other hand we define positive bending moment M as inward, and positive displacement δ as outward, irrespective of the viewer's location. As a consequence the displacement misalignments in Equation (19) involve the difference of the membrane displacements, the rotational misalignments in Equation (21) involve the sum of the membrane rotations. The foregoing is in accordance with the sign conventions introduced by Horvay and Clausen.[6]

It is readily seen that to eliminate the misalignments, edge shears $\mathcal{H}_2$, $\mathcal{H}_{1u}$, $\mathcal{H}_{1\ell}$, $\mathcal{H}_0$ and edge moments $\mathcal{M}_2$, $\mathcal{M}_{1u}$, $\mathcal{M}_{1\ell}$, $\mathcal{M}_0$ must be developed (1 u = upper edge of Zone 1, 1ℓ = lower edge of Zone 1) which are in equilibrium

$$\mathcal{M}_2 = \mathcal{M}_1, \mathcal{H}_2 + \mathcal{H}_{1u} = 0$$
$$\mathcal{M}_1 = \mathcal{M}_0, \mathcal{H}_{1\ell} + \mathcal{H}_0 = 0 \qquad (22)$$

and which give rise to deformations at the upper edge of Zone 1

$$\bar{\delta}_{1u} = \frac{1}{2} f_1 \ell_1 (-\mathcal{M}_{1u} + \mathcal{H}_{1u}\ell_1), \quad \bar{\chi}_{1u} = f_1 (\mathcal{M}_{1u} - \frac{1}{2}\mathcal{H}_{1u}\ell_1) \qquad (23)$$

Similar expressions $\bar{\delta}_{1\ell}$, $\bar{\chi}_{1\ell}$; $\bar{\delta}_2$, $\bar{\chi}_2$; $\bar{\delta}_0$, $\bar{\chi}_0$ also hold at the lower edge of Zone 1, at the lower edge of Zone 2, and at the upper edge of Zone 0, respectively. The bar above the letter denotes the "edge value" of deformations δ and χ ; a change from Latin to script letter signifies the edge value of moment and force M_x and H.

In the foregoing

$$\ell_1 = (4\beta/K)^{1/4} \qquad (24a)$$

is the "attenuation length" of Zone 1 of the shell, where

6. "Membrane and bending analysis of axisymmetrically loaded axisymmetrical shells," by G. Horvay and I. M. Clausen. J.A.M., in press.

$$K = \kappa + k \tag{24b}$$

denotes the combined spring restraint provided by the shell wall and the soil,

$$D = Eh^3/12(1 - \mu^2) \tag{24c}$$

is the bending stiffness of the shell, and

$$f_1 = \ell_1 / D \tag{24d}$$

is the "flexibility" of the shell.

For shell Zones 2 and 0 the corresponding quantities are obtained by substituting into Equation (24b) values of $\kappa = 0$ and $\kappa = \infty$, respectively.

From the four continuity requirements

$$\begin{aligned} \bar{\delta}_{1u} - \bar{\delta}_2 &= \delta^*_{21}, \quad \bar{X}_{1u} + \bar{X}_2 = 0 \\ \bar{\delta}_0 - \bar{\delta}_{1\ell} &= \delta^*_{10}, \quad \bar{X}_0 + \bar{X}_{1\ell} = 0 \end{aligned} \tag{25}$$

and using the four equilibrium Equations (22), we solve for the 8 unknown edge reactions, and find in terms of the ratio

$$\beta = \ell_1/\ell_2 = (K_2/K_1)^{1/4} = (1 + \rho)^{-1/4} \tag{26}$$

the values

$$\begin{aligned} m_2 = m_{1u} &= -\frac{2(1 - \beta)\rho}{(1 + \beta + \beta^2 + \beta^3)(1 + \rho)} \cdot \frac{\delta_p}{f_2 \ell_2} \\ h_2 = -h_{1u} &= -\frac{4\rho}{(1 + \beta + \beta^2 + \beta^3)(1 + \rho)} \cdot \frac{\delta_p}{f_2 \ell_2^2} \\ m_{1\ell} = m_0 &= -\frac{2}{1 + \rho} \cdot \frac{\delta_p}{f_1 \ell_1} \\ h_{1\ell} = -h_0 &= -\frac{4}{1 + \rho} \cdot \frac{\delta_p}{f_1 \ell_1^2} \end{aligned} \tag{27}$$

Deformations and Stresses Produced by Edge Loading

The edge actions m_{1u}, h_{1u} manifest themselves, in accordance with Table 2[6] in the radial displacement

$$\delta_{1u} = \frac{1}{2} f_1 \ell_1 e^{-n_{1u}} \left[m_{1u} \sqrt{2} \sin(n_{1u} - \pi/4) + h_{1u} \ell_1 \cos n_{1u} \right] \tag{28a}$$

and in the meridional bending moment

$$M_{x,1u} = e^{-n_{1u}} \left[m_{1u} \sqrt{2} \cos(n_{1u} - \pi/4) - h_{1u} \ell_1 \sin n_{1u} \right] \tag{28b}$$

in Zone 1, at a distance $n_{1u}\ell_1$ from interface $\overline{21}$. Similar relations also hold for the quantities derived from $m_2, \ldots, h_0$. Knowing δ and M_x we obtain the meridional bending stress from

$$\sigma_x = \mp 6\, M_x/h^2 \tag{29a}$$

and the hoop stress from

$$\sigma_\theta = E\delta/R \mp 6\mu M_x/h^2 \tag{29b}$$

The upper sign refers to inner and the lower sign to outer fiber stress.

Resultant Stresses and Displacements

Referring to the effects of edge-load actions $\mathcal{M}_2, \ldots, \mathcal{H}_0$ listed in the previous section by subscript e, we determine the resultant deformation and stresses in Zone 1 of the shell taking

$$\begin{aligned} \delta_1 &= \delta_{1m} + \delta_{1e} \\ \sigma_{x1} &= \sigma_{x1m} + \sigma_{x1e} \\ \sigma_{\theta 1} &= \sigma_{\theta 1m} + \sigma_{\theta 1e} \end{aligned} \tag{30}$$

Corresponding quantities in the other zones are similarly formed. Expressions for δ_e, σ_{xe}, $\sigma_{\theta e}$ were listed in the preceding section, and expressions for δ_m, σ_{xm}, $\sigma_{\theta m}$ were listed in the section on "Membrane State."

We plot the resultant deformation δ and the resultant stress σ_x, so obtained throughout the shell, in Figs. 5 and 6 versus distance from interface, for ρ = 0, 1, 10, ∞. Our assumption that Zone 1 is several (at least 3) attenuation lengths long insures that what happens at one interface has no effect on the opposite interface of this zone.

From the curve of σ_x shown on Fig. 6, and from a similar curve (not shown) for σ_θ, we derive the composite Fig. 7, plotting the maxima and minima of the respective stresses. For instance, we see from Fig. 6 that the maximum value which the meridional stress reaches in Zone 1 for $\rho = 1$ is $\sigma_{x\,max} = 1.26\,\sigma_p$ in the inner fiber at interface $\overline{10}$, and $\sigma_{x\,max} = 0.66\,\sigma_p$ in the inner fiber at 0.7ℓ distance from interface $\overline{21}$. These two values are plotted at $\rho = 1$ on the $\sigma_{x\overline{10}i}$ and the $\sigma_{x\overline{21}i}$ curves.

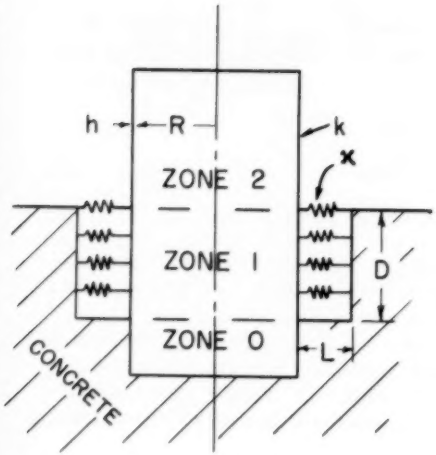

Fig. 1

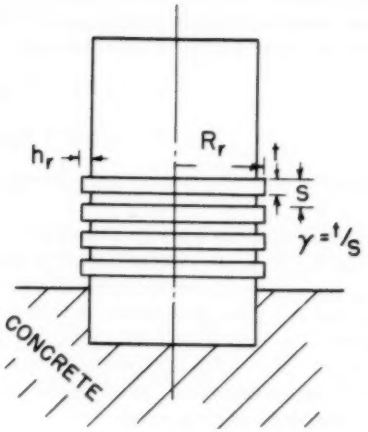

Fig. 2

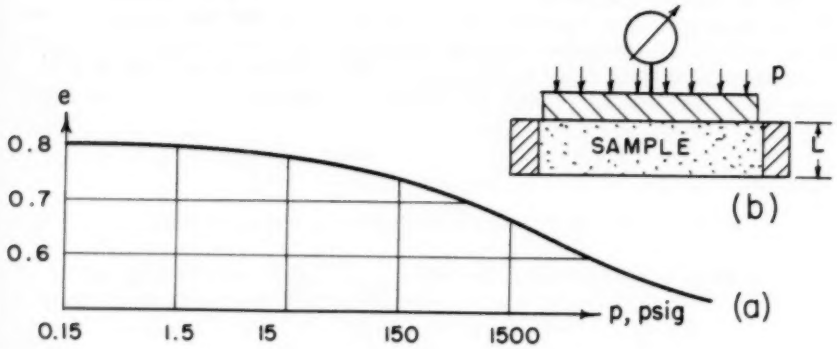

Fig. 3

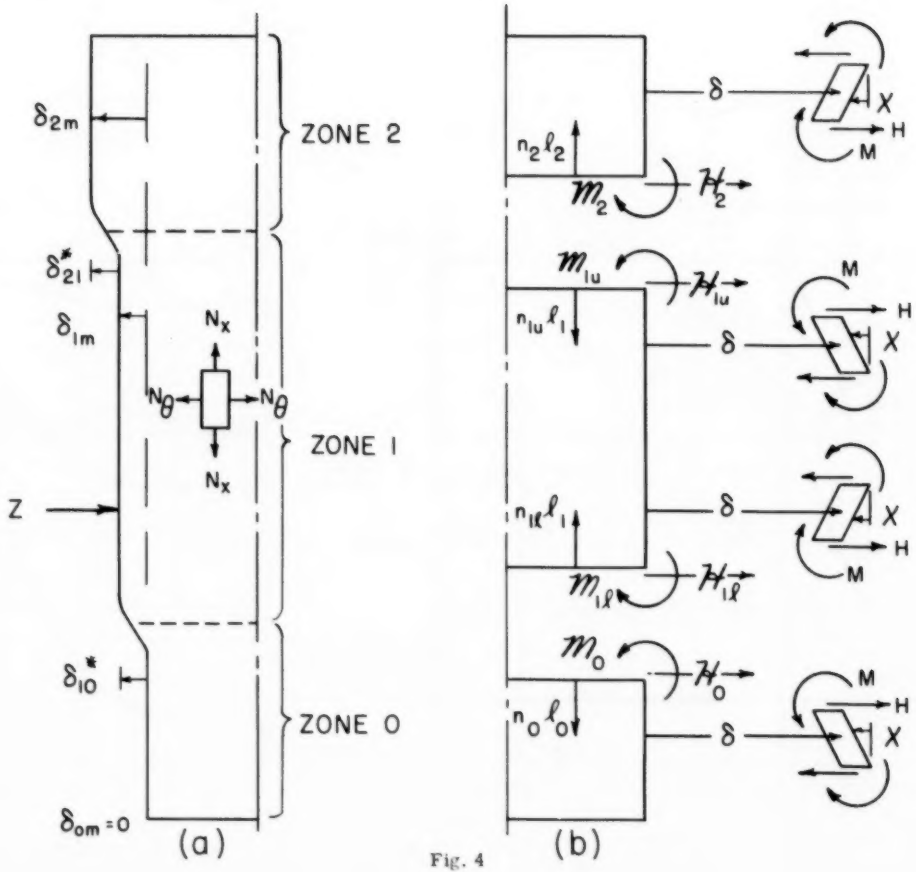
δ2m
ZONE 2
δ*21
δ1m
Nx
Nθ
Nθ
Nx
ZONE 1
Z
δ*10
ZONE 0
δom = 0
(a)
δ
X
H
M
n2 l2
m2
H2
m1u
H1u
n1u l1
n1l l1
m1l
H1l
m0
H0
n0 l0
(b)

Fig. 4

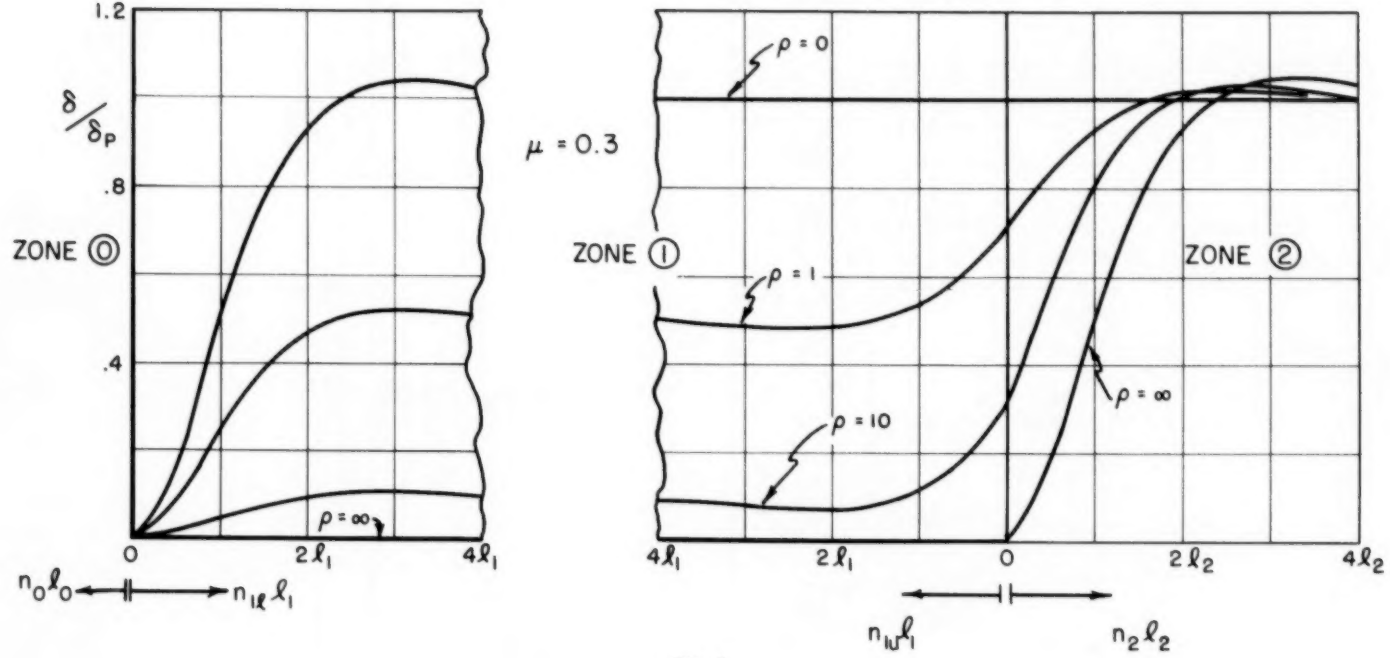
1.2
δ/δP
.8
ZONE ⓪
.4
ρ = ∞
0
2ℓ1
4ℓ1
n0ℓ0
n1ℓ1
μ = 0.3
ρ = 0
ZONE ①
ρ = 1
ZONE ②
ρ = 10
ρ = ∞
4ℓ1
2ℓ1
0
2ℓ2
4ℓ2
n1ℓ1
n2ℓ2

677-10

Fig. 5

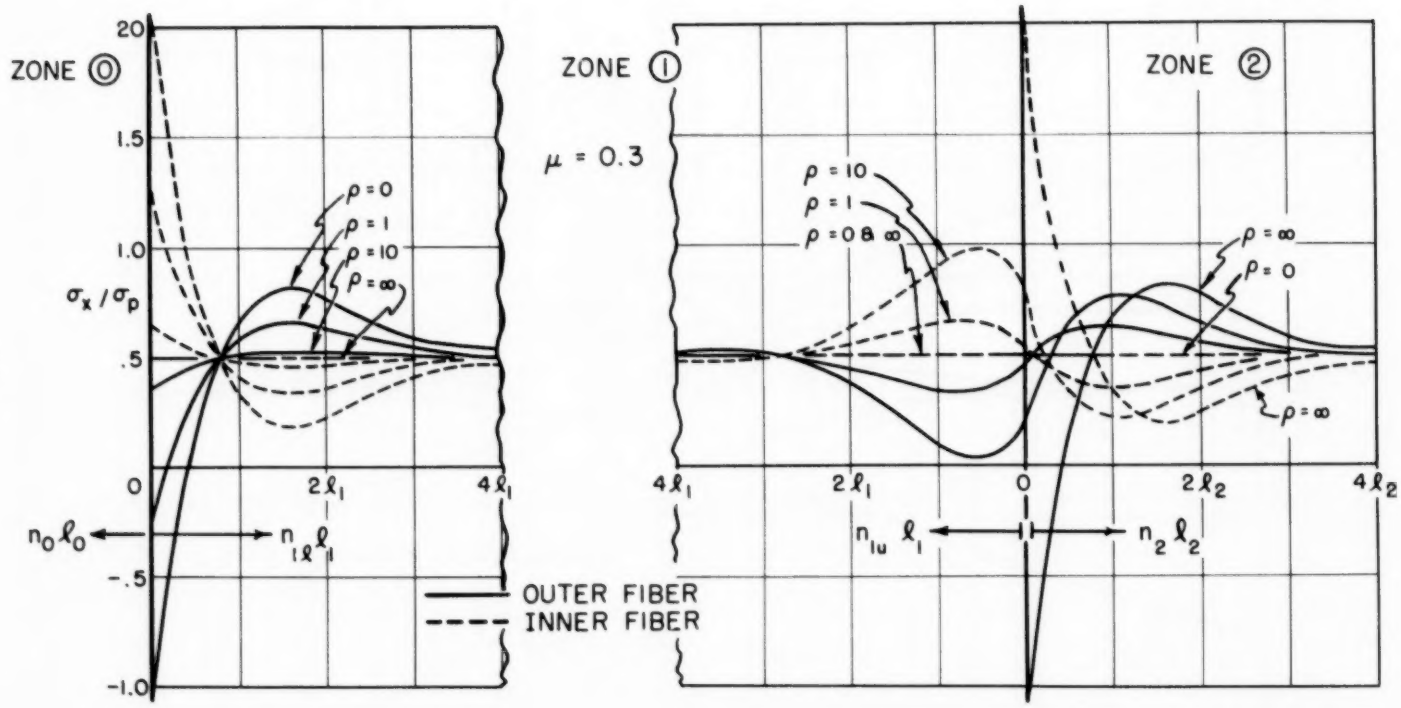
ZONE ⓪
ZONE ①
ZONE ②
μ = 0.3
σx / σp
ρ = 0
ρ = 1
ρ = 10
ρ = ∞
ρ = 10
ρ = 1
ρ = 0.8 ∞
ρ = ∞
ρ = 0
ρ = ∞
20
1.5
1.0
.5
0
-.5
-1.0
2ℓ1
4ℓ1
4ℓ1
2ℓ1
0
2ℓ2
4ℓ2
n0ℓ0
n1ℓ1
nluℓ1
n2ℓ2
OUTER FIBER
INNER FIBER

Fig. 6

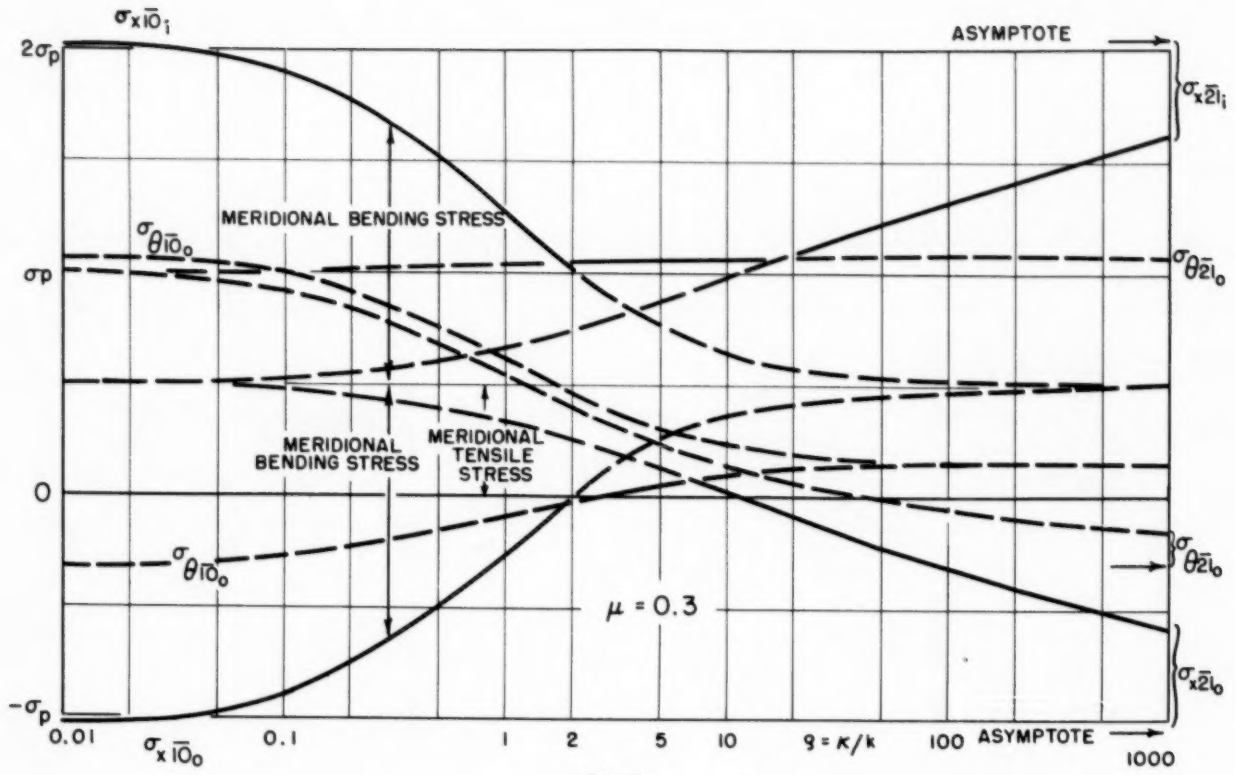
$\sigma_{x\bar{1}0_i}$
ASYMPTOTE
$2\sigma_p$
$\sigma_{x\bar{2}1_i}$
MERIDIONAL BENDING STRESS
$\sigma_{\theta\bar{1}0_o}$
σp
$\sigma_{\theta\bar{2}1_o}$
MERIDIONAL BENDING STRESS
MERIDIONAL TENSILE STRESS
0
$\sigma_{\theta\bar{1}0_o}$
$\sigma_{\theta\bar{2}1_o}$
$\mu = 0.3$
$\sigma_{x\bar{2}1_o}$
$-\sigma_p$
0.01
$\sigma_{x\bar{1}0_o}$
0.1
1
2
5
10
$\varrho = \kappa/k$
100
ASYMPTOTE
1000

Fig. 7

PROCEEDINGS-SEPARATES

The technical papers published in the past year are presented below. Technical-division sponsorship is indicated by an abbreviation at the end of each Separate Number, the symbols referring to: Air Transport (AT), City Planning (CP), Construction (CO), Engineering Mechanics (EM), Highway (HW), Hydraulics (HY), Irrigation and Drainage (IR), Power (PO), Sanitary Engineering (SA), Soil Mechanics and Foundations (SM), Structural (ST), Surveying and Mapping (SU), and Waterways (WW) divisions. For titles and order coupons, refer to the appropriate issue of "Civil Engineering" or write for a cumulative price list.

VOLUME 80 (1954)

APRIL: 428(HY)[c], 429(EM)[c], 430(ST), 431(HY), 432(HY), 433(HY), 434(ST).

MAY: 435(SM), 436(CP)[c], 437(HY)[c], 438(HY), 439(HY), 440(ST), 441(ST), 442(SA), 443(SA).

JUNE: 444(SM)[e], 445(SM)[e], 446(ST)[e], 447(ST)[e], 448(ST)[e], 449(ST)[e], 450(ST)[e], 451(ST)[e], 452(SA)[e], 453(SA)[e], 454(SA)[e], 455(SA)[e], 456(SM)[e].

JULY: 457(AT), 458(AT), 459(AT)[c], 460(IR), 461(IR), 462(IR), 463(IR)[c], 464(PO), 465(PO)[c].

AUGUST: 466(HY), 467(HY), 468(ST), 469(ST), 470(ST), 471(SA), 472(SA), 473(SA), 474(SA), 475(SM), 476(SM), 477(SM), 478(SM)[c], 479(HY)[c], 480(ST)[c], 481(SA)[c], 482(HY), 483(HY).

SEPTEMBER: 484(ST), 485(ST), 486(ST), 487(CP)[c], 488(ST)[c], 489(HY), 490(HY), 491(HY)[c], 492(SA), 493(SA), 494(SA), 495(SA), 496(SA), 497(SA), 498(SA), 499(HW), 500(HW), 501(HW)[c], 502(WW), 503(WW), 504(WW)[c], 505(CO), 506(CO)[c], 507(CP), 508(CP), 509(CP), 510(CP), 511(CP).

OCTOBER: 512(SM), 513(SM), 514(SM), 515(SM), 516(SM), 517(PO), 518(SM)[c], 519(IR), 520(IR), 521(IR), 522(IR)[c], 523(AT)[c], 524(SU), 525(SU)[c], 526(EM), 527(EM), 528(EM), 529(EM), 530(EM)[c], 531(EM), 532(EM)[c], 533(PO).

NOVEMBER: 534(HY), 535(HY), 536(HY), 537(HY), 538(HY)[c], 539(ST), 540(ST), 541(ST), 542(ST), 543(ST), 544(ST), 545(SA), 546(SA), 547(SA), 548(SM), 549(SM), 550(SM), 551(SM), 552(SA), 553(SM)[c], 554(SA), 555(SA), 556(SA), 557(SA).

DECEMBER: 558(ST), 559(ST), 560(ST), 561(ST), 562(ST), 563(ST)[c], 564(HY), 565(HY), 566(HY), 567(HY), 568(HY)[c], 569(SM), 570(SM), 571(SM), 572(SM)[c], 573(SM)[c], 574(SU), 575(SU), 576(SU), 577(SU), 578(HY), 579(ST), 580(SU), 581(SU), 582(Index).

VOLUME 81 (1955)

JANUARY: 583(ST), 584(ST), 585(ST), 586(ST), 587(ST), 588(ST), 589(ST)[c], 590(SA), 591(SA), 592(SA), 593(SA), 594(SA), 595(SA)[c], 596(HW), 597(HW), 598(HW)[c], 599(CP), 600(CP), 601(CP), 602(CP), 603(CP), 604(EM), 605(EM), 606(EM)[c], 607(EM).

FEBRUARY: 608(WW), 609(WW), 610(WW), 611(WW), 612(WW), 613(WW), 614(WW), 615(WW), 616(WW), 617(IR), 618(IR), 619(IR), 620(IR), 621(IR)[c], 622(IR), 623(IR), 624(HY)[c], 625(HY), 626(HY), 627(HY), 628(HY), 629(HY), 630(HY), 631(HY), 632(CO), 633(CO).

MARCH: 634(PO), 635(PO), 636(PO), 637(PO), 638(PO), 639(PO), 640(PO), 641(PO)[c], 642(SA), 643(SA), 644(SA), 645(SA), 646(SA), 647(SA)[c], 648(ST), 649(ST), 650(ST), 651(ST), 652(ST), 653(ST), 654(ST)[c], 655(SA), 656(SM)[c], 657(SM)[c], 658(SM)[c].

APRIL: 659(ST), 660(ST), 661(ST)[c], 662(ST), 663(ST), 664(ST)[c], 665(HY)[c], 666(HY), 667(HY), 668(HY), 669(HY), 670(EM), 671(EM), 672(EM), 673(EM), 674(EM), 675(EM), 676(EM), 677(EM), 678(HY).

c. Discussion of several papers, grouped by Divisions.
e. Presented at the Atlantic City (N.J.) Convention in June, 1954.

AMERICAN SOCIETY OF CIVIL ENGINEERS

OFFICERS FOR 1955

PRESIDENT

WILLIAM ROY GLIDDEN

VICE-PRESIDENTS

Term expires October, 1955:
ENOCH R. NEEDLES
MASON G. LOCKWOOD

Term expires October, 1956:
FRANK L. WEAVER
LOUIS R. HOWSON

DIRECTORS

Term expires October, 1955:
CHARLES B. MOLINEAUX
MERCEL J. SHELTON
A. A. K. BOOTH
CARL G. PAULSEN
LLOYD D. KNAPP
GLENN W. HOLCOMB
FRANCIS M. DAWSON

Term expires October, 1956:
WILLIAM S. LaLONDE, JR.
OLIVER W. HARTWELL
THOMAS C. SHEDD
SAMUEL B. MORRIS
ERNEST W. CARLTON
RAYMOND F. DAWSON

Term expires October, 1957:
JEWELL M. GARRELTS
FREDERICK H. PAULSON
GEORGE S. RICHARDSON
DON M. CORBETT
GRAHAM P. WILLOUGHBY
LAWRENCE A. ELSENER

PAST-PRESIDENTS

Members of the Board

WALTER L. HUBER
DANIEL V. TERRELL

EXECUTIVE SECRETARY

WILLIAM N. CAREY

ASSOCIATE SECRETARY

WILLIAM H. WISELY

TREASURER

CHARLES E. TROUT

ASSISTANT SECRETARY

E. L. CHANDLER

ASSISTANT TREASURER

CARLTON S. PROCTOR

PROCEEDINGS OF THE SOCIETY

HAROLD T. LARSEN
Manager of Technical Publications

DEFOREST A. MATTESON, JR.
Editor of Technical Publications

PAUL A. PARISI
Assoc. Editor of Technical Publications

COMMITTEE ON PUBLICATIONS

SAMUEL B. MORRIS, *Chairman*

JEWELL M. GARRELTS, *Vice-Chairman*

GLENN W. HOLCOMB
OLIVER W. HARTWELL
ERNEST W. CARLTON
DON M. CORBETT